Tribochemistry of Phosphoric Acid Sheared between Quartz Surfaces: A Reactive Molecular Dynamics Study

ARTICLE *in* THE JOURNAL OF PHYSICAL CHEMISTRY C · NOVEMBER 2013

Impact Factor: 4.77 · DOI: 10.1021/jp406360u

7 AUTHORS, INCLUDING:

Tian-Bao Ma
Tsinghua University
25 PUBLICATIONS **272** CITATIONS
SEE PROFILE

Yuanzhong Hu
Tsinghua University
118 PUBLICATIONS **1,727** CITATIONS
SEE PROFILE

Adri C.T. van Duin
Pennsylvania State University
362 PUBLICATIONS **8,239** CITATIONS
SEE PROFILE

THE JOURNAL OF PHYSICAL CHEMISTRY C

Article

pubs.acs.org/JPCC

Tribochemistry of Phosphoric Acid Sheared between Quartz Surfaces: A Reactive Molecular Dynamics Study

Da-Chuan Yue,[†] Tian-Bao Ma,*[,†] Yuan-Zhong Hu,[†] Jejoon Yeon,[‡] Adri C. T. van Duin,[‡] Hui Wang,[†] and Jianbin Luo[†]

[†]State Key Laboratory of Tribology, Tsinghua University, Beijing 100084, China

[‡]Department of Mechanical and Nuclear Engineering, Pennsylvania State University, University Park, Pennsylvania 16802, United States

ABSTRACT: Tribochemical processes have profound consequences on tribological performance. In the present paper, the tribochemical mechanism of low friction state in the silica/phosphoric acid system is elucidated by reactive molecular dynamics (ReaxFF) simulations. The friction coefficient is found having strong positive correlation with the number of interfacial hydrogen bonds, which suggests that a weaker interfacial hydrogen bond network would favor a lower friction. The friction reduction mechanisms have been analyzed in two temperature regimes: For 300 ≤ T ≤ 600 K, no indication of tribochemical reaction is observed, and the friction coefficient decreases because of the accelerated molecular rotational and translational motion and the corresponding weakened hydrogen bond network. For 800 K ≤ T ≤ 1400 K, the occurrence of tribochemical reactions leads to a clustering and polymerization of the phosphoric acid molecules and generation of a considerable quantity of water molecules distributed mainly in the sliding interface which could act as lubricant, and a low friction state is reached with a friction coefficient of 0.02.

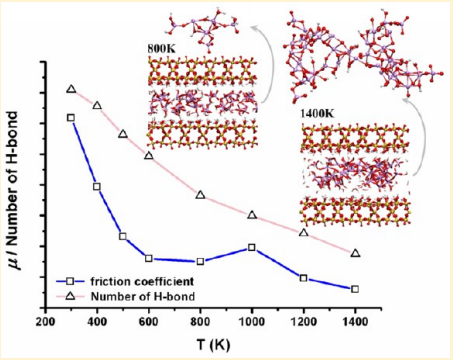

1. INTRODUCTION

In tribology, the science of surfaces in relative motion, the behavior of phosphates under extreme conditions is of tremendous interest. It stems from the excellent antiwear property of zinc phosphates. As the most common antiwear additives, zinc dialkyldithiophosphates (ZDDPs), which have the chemical formula $Zn[S_2P(OR)_2]_2$, have been used for over 60 years.[1] Up to now, people find in both experiments and simulations that the zinc phosphate film formed in tribochemical reaction plays a crucial role in the antiwear mechanism.[2−4] Nevertheless, despite decades of research on the antiwear property of phosphates,[3,4] to the best of our knowledge, there were few works focused on their friction reduction capability. In this context, the recent experimental effort made by Li et al.[5] which realizes a superlubricity state in the silica/phosphoric acid system is remarkable. The so-called superlubricity, which was proposed by Hirano and Shinjo at the beginning of the 1990s,[6,7] is a lubrication regime in which the friction between two contacting surfaces nearly vanished. It is generally thought that when the friction coefficient is below 0.01, the lubricating state is considered in the superlubricity regime.[8]

Noticeably, in Li's experiment, there is significant tribochemical reaction in the running-in period, during which the friction coefficient decreases drastically to below 0.01, and a gel-like film is formed on both the sliding track and the countersurface. This phenomenon indicates that the tribochemical reaction plays an important role in this superlubricity system. In several theoretical and experimental studies, efforts have also been made to investigate tribochemical reactions in the context of lubrication in other systems.[9−15] Shedding light on the silica/phosphoric acid system from an atomistic level would thus greatly assist building up a tribochemical theory of superlubricity, which has attracted tremendous interest in the past decade.[16−20] While clarifying the molecular mechanism of tribochemical processes still presents a challenge to experiments due to the complexity of the friction system, computer simulation has proven to be an effective means to study tribochemistry mechanism from the molecular level.[21,22]

First-principles molecular dynamics simulation is expected to be an ideal method to explore the chemical process in a sliding friction system. Recently, it has been carried out to study the nature of the tribochemical reaction under boundary lubrication conditions.[23−28] In an impressive work by Mosey et al., a Car−Parrinello first-principles molecular dynamics simulation is adopted to study the formation mechanism of antiwear film from zinc phosphate lubricant additive under extreme pressure.[1,23] Unfortunately, the computational cost of the first-principles molecular dynamics is huge for a large realistic system. There is also a trend in recent years on the development and application of reactive force fields which can account for changes in chemical bonding during reactions

Received: June 27, 2013
Revised: November 20, 2013
Published: November 20, 2013

in a computationally efficient way.[29−41] At first, the reactive force fields have been successfully applied to the tribochemistry of chemically modified diamond surfaces in sliding contact.[29−31] In the following studies of tribological properties of self-assembled monolayer (SAM), load and shear induced polymerization between chains have been observed.[32−34] Recently, the shear-induced graphitization of amorphous carbon films was observed which could lead to a very low friction.[37]

ReaxFF is a new general bond-order-dependent force field based on extensive ab initio calculations.[42,43] The excellent combination between good accuracy for both reaction energies and reaction barriers and reasonable computational cost makes the ReaxFF method ideally suited for the description of complex reacting systems using molecular dynamics. By now, ReaxFF has been successfully used to simulate various materials,[42−47] interfaces,[48−53] and friction processes.[38−41] Moreover, this approach can be easily extended to any molecular system of any class of compounds.[42]

In this paper, we aim at unraveling the mechanism of superlubricity induced by tribochemical reaction of the silica/phosphoric acid system from an atomistic level. It is well-known that the temperature increase caused by energy dissipation will activate interfacial atoms,[54] thereby facilitating the interfacial chemical reaction. Moreover, at the microscopic asperities of contact, flash temperature—one of the key features in tribological systems—can be close to or even exceed the theoretical melting point of the surface material.[1,55] So temperature is the key factor to be considered in this paper, a series of system temperatures are used to study the tribochemical response of the silica/phosphoric acid system.

2. METHODS AND MODELS

2.1. ReaxFF Method. The forces between atoms are derived from ReaxFF, a sophisticated reactive force field developed during the past decade. The ReaxFF method, allowing chemical bond to break and form, is an empirical force field which uses a bond order/bond distance relationship to describe atomic interactions. Given that chemical reactions and large geometrical variations can change the charge distribution dramatically. A charge equilibration method (QEq) is utilized to calculate the charge distributions based on geometry and connectivity throughout the course of the simulation. The parameters involved in the ReaxFF potential were derived by fitting against a training set consist of both quantum mechanics (QM) and experimental results.

To describe the various interaction among phosphoric acid[47] and hydroxylated silica surfaces[43,49] during lubrication, optimization of the force field is essential to acquire proper parameter values. First, the parameters to describe phosphoric acid and bulk silica have been merged to build a base force field. Then, parameters for various interactions among two materials were optimized by comparing DFT calculation data with ReaxFF result. The optimization process of the phosphate parameters includes, among others, comparison against DFT values for the vibration frequencies of H_3PO_4, charge distribution, dissociation of the single/double bond of P−O bond, and bond angle of P−O−H bond.

The parameters for deprotonation of the H_3PO_4, H_2PO_4, and HPO_4 also have been compared and fitted against DFT values. This training set includes the reaction pathway of proton transfer process, allowing ReaxFF to realistically model the proton dynamics. Specially, deprotonation of H_3PO_4 included due to its abundance in phosphoric acid group

$$H_3PO_4 + H_2O \rightarrow H_2PO_4^- + H_3O^+ \quad (1)$$

The proton donation of H_3PO_4 to the water molecules has a very small energy barrier. The ReaxFF parameters were optimized to have similar level of activation energy compared to DFT calculations. Parameters for interaction with water and hydronium related are fitted together, inducing ReaxFF to simulate phosphoric acid group properly interacts during reaction related with proton atoms.

ReaxFF was also trained against DFT results for phosphate dimerization. By fitting dimerization related parameters, ReaxFF can also describe the long-range interaction between phosphoric acid molecules. In addition, parameters for hydrolysis reactions including H_3PO_4 have been studied as follows:

$$H_3PO_4 + H_2O \leftrightarrow P(OH)_5 \quad (2)$$

Results from the optimized force field and DFT simulation are in good agreement—ReaxFF is typically within 2 kcal/mol of the DFT result, indicating that ReaxFF can accurately describe these hydrolysis reactions.

As described in Queneville et al.,[50] these phosphate ReaxFF parameters[47] were subsequently merged with the silica force field by training the Si−O−P angle parameters against reaction energies between H_3PO_4 and $Si(OH)_4$. In their work, these parameters—also used in the present work—have been successfully applied to describe interaction between silica surface and phosphoric acid derivative.[50]

2.2. Model. For the simulation, quartz $(10\bar{1}0)$ substrate is chosen, with dimensions 29.460 Å × 21.608 Å × 8.504 Å. The dangling bonds on the quartz surfaces are terminated with hydroxyl groups to form chemically passivated surfaces. A sliding couple model for friction calculations was constructed by bringing two quartz substrates into a face-to-face structure, forming an interface between the two surfaces where the friction occurred. 44 phosphoric acid molecules were inserted randomly to separate two surfaces. Although the phosphoric used in experiments should be a mixture of orthophosphoric, polyphosphoric acid, and water, purely orthophosphoric acid molecules are used in the present simulation to learn the tribochemical processes and their contribution to friction reduction for a fundamental research. Prior to the friction simulations, this system was well relaxed at 300 K, primarily to remove short contacts in the interface related to the random placement of phosphoric acid molecules. The constructed model is presented in Figure 1.

It is demonstrated by Liu et al.[56] that the chemical state of the interface is strongly dependent on time. It is worth finding out whether the phosphoric acid reacts with the surface before sliding. In a previous study,[50] it has been demonstrated using both reactive molecular dynamics simulations and quantum chemical studies that the phosphoric acid derivative can hardly react with a highly passivated silica surface. The binding of phosphoric acid derivative to the hydroxylated silica surface was found to occur through a combination of van der Waals interactions and hydrogen bonds. In our cases, the highly passivated silica surface and strong acidic condition are used in both present simulation and the related experiment.[5] Noteworthily, the strong acidic condition could further favor surface passivation. Here we assume that the dangling bond is always passivated in such a strong acidic condition (which should be

dx.doi.org/10.1021/jp406360u | J. Phys. Chem. C 2013, 117, 25604−25614

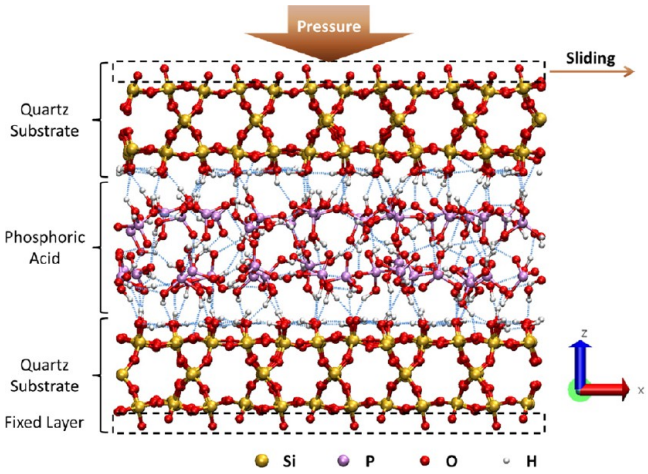

Figure 1. Schematic figure of the model used in friction simulations. This figure was rendered using VMD.[57] Silicon, phosphorus, oxygen, and hydrogen are colored in yellow, purple, red, and white, respectively. The blue dotted lines represent hydrogen bonds. We defined the hydrogen bond by using a geometrical criterion: a cutoff distance of 3.5 Å between a donor atom; an acceptor atom and a cutoff angle of 45° for the hydrogen donor−acceptor angle.[50]

the case on experimental time scales). Therefore, in our cases the interfacial interaction is dominated by hydrogen bonds, and we could claim that after such a relaxation process we could get the appropriate configuration before sliding.

2.3. Friction Simulation. The friction MD simulation was performed with the LAMMPS code,[58] using a Verlet algorithm to integrate the trajectories and a time step of 0.25 fs. As shown in Figure 1, an external normal pressure of 600 MPa, which is consistent with the experimental pressure of Li et al.,[5] was applied on the top layer of the upper substrate along the $-z$ direction. And the sliding simulation was carried out as follows: under the periodic boundary condition, the top layer of the upper substrate was forced sliding with a constant velocity of 100 m/s, i.e., 1 Å/ps, along the sliding direction (x direction), whereas the bottom layer of the lower substrate was completely frozen throughout the whole simulation. The next two layers, which are below the top layer and above the bottom layer, respectively, are coupled to a Langevin thermostat in order to control the system temperature,[59] with a temperature damping constant of 100 fs. The remaining atoms in the box were free of constraints; thus, they can move freely according to the forces. To mimic the aforementioned extreme interfacial temperature conditions on tribochemical reaction, we perform 8 MD simulations with system temperatures varying from 300 to 1400 K. In each case, at the beginning of the sliding, system temperature was raised from an initial temperature of 300 K to target temperatures of 300, 400, 500, 600, 800, 1000, 1200, and 1400 K. The target temperatures are chosen by considering two factors: (1) the significance of flash temperature to tribochemical processes, which can be close to or even slightly exceed the melting point of the surface material; (2) the acceleration of tribochemical reactive processes in MD simulations due to the time-scale limitation.

2.4. Cumulative Averaged Friction Coefficient. The friction coefficient was calculated from the force acting on the fixed substrate atoms. In detail, the cumulative averaged friction coefficient μ_{ave} was calculated from $F_{x\text{-averaged}}$ and $F_{z\text{-averaged}}$ as follows:[60]

$$\mu_{ave} = \frac{F_{x\text{-averaged}}}{F_{z\text{-averaged}}} \tag{3}$$

$$F_{x\text{-averaged}} = \frac{\sum_i F_x}{i} \tag{4}$$

$$F_{z\text{-averaged}} = \frac{\sum_i F_z}{i} \tag{5}$$

Here, i is the number of steps for every step, and F_x and F_z represent the instantaneous horizontal and perpendicular forces with respect to the fixed layer of the lower substrate, respectively. So $F_{x\text{-averaged}}$ and $F_{z\text{-averaged}}$ are the averaged values of the sums of the horizontal and perpendicular forces, respectively.

2.5. Reorientational Correlation Time. In order to calculate reorientational correlation time, we followed the procedure already used for the reorientation dynamics of benzene and water.[53,61−65] The framework of phosphoric acid molecule consists of one central phosphorus atom surrounded by four oxygen atoms in a tetrahedral arrangement, so all four PO bonds are almost symmetrically equivalent. Considering this, we define a unit vector $\mu(t)$ whose direction is the orientation of the PO bond at time t. Hence, the rotation of phosphoric acid molecules can be characterized by the time-evolution of the unit vector $\mu(t)$ for PO group. The reorientation correlation function of the unit vector $\mu(t)$ is defined as follows:

$$C(t) = \langle P_1[\mu(t)\mu(0)]\rangle \tag{6}$$

where P_1 is the first rank Legendre polynomial. Generally speaking, the correlation function, especially for molecular liquids, is often found to follow an exponential decay after some short-time features.[62] And the decay of the correlation function is fitted well by the Kohlrausch−Williams−Watts (KWW) stretched exponential function $\exp[-(t/\tau)^\gamma]$.[62,64] The time integral of the correlation function yields the corresponding correlation time τ_μ, which is analytical for a stretched exponential

$$\tau_\mu = \int_0^\infty \exp[-(t/\tau)^\gamma]\, dt = \frac{\tau}{\gamma}\Gamma\left(\frac{1}{\gamma}\right) \tag{7}$$

where $\Gamma(x)$ is the gamma factorial function.

2.6. Mean-Squared Displacement (MSD). To study the translational diffusion dynamics, the diffusion coefficient is computed from the MSD of the phosphoric acid molecules as follows:

$$\mathrm{MSD}(t) = \frac{1}{T}\sum_{t_0=1}^{T}\frac{1}{N}\sum_{i=1}^{N}(r_i(t_0+t) - r_i(t_0))^2 \tag{8}$$

$$D = \frac{1}{2n}\lim_{t\to\infty}\frac{d\mathrm{MSD}(t)}{dt} \tag{9}$$

where r_i denotes the position vector of the ith atom, t is the time interval, N is the number of atoms, T is the total number of time steps averaged over, D is the diffusion coefficient, and n is the degree of dimensions. A best linear fit to MSD gives the value of D.

dx.doi.org/10.1021/jp406360u | J. Phys. Chem. C 2013, 117, 25604−25614

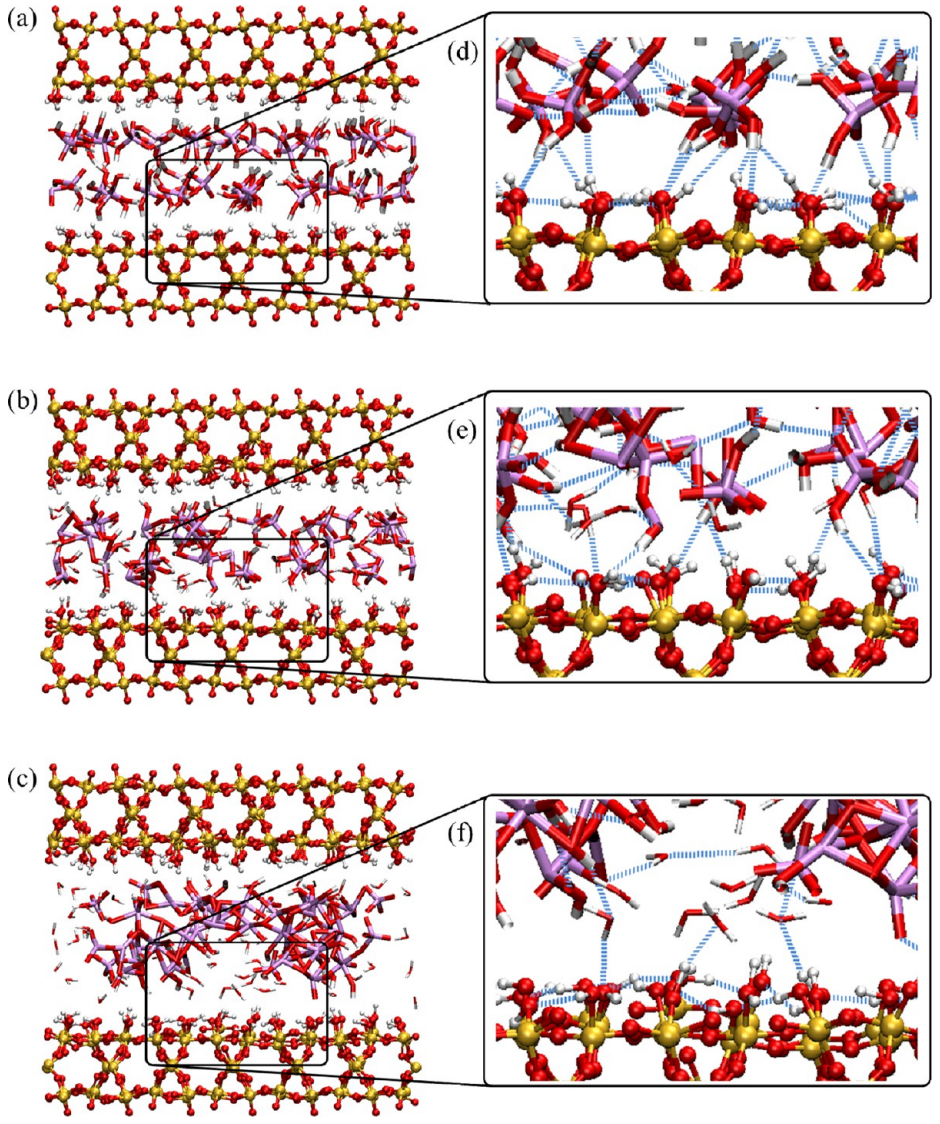

Figure 2. Last snapshots of sliding simulations at various temperatures: (a) 300, (b) 800, and (c) 1400 K. The color scheme is the same as that described in the caption of Figure 1. The ball-and-stick representation shows the quartz substrate atoms. The stick-only representation shows the lubricant molecules which would be phosphoric acid, poly(phosphoric acid), and water. For distinguishability, the waters are represented with thin sticks, whereas the phosphoric acid and poly(phosphoric acid) are represented with thick sticks. For clarity, the hydrogen bonds are omitted. Partial enlarged detail views: (d) 300, (e) 800, and (f) 1400 K. The hydrogen bond representation is the same as that described in the caption of Figure 1.

3. RESULTS AND DISCUSSION

3.1. Sliding Friction Behaviors and Interfacial Interactions. From the snapshots of these simulations, we find that there do exist tribochemical reactions, but they are highly temperature dependent; i.e., the tribochemical reactions only occur at relatively higher temperatures ($T > 600$ K). To provide a direct description of the evolution of the interfacial structure, the last snapshots of sliding simulations at different temperatures are shown in Figure 2a–c. The ball-and-stick representation shows the quartz substrate atoms, and the stick-only representation shows the lubricant molecules. Figure 2a shows that during the sliding process at 300 K the phosphoric acid molecules will basically keep the original structural integrity as a tetrahedral framework and form a layered structure due to surface confinement. In fact, this situation remains unchanged in the lower temperature range($300 \leq T \leq 600$ K). However, at system temperature of 800 K, phosphoric acid molecules do not keep their original molecular structure anymore but connect to each other with chemical bonds, along with the production of water molecules, as shown in Figure 2b. For distinguishability, the water molecules are represented with thin sticks, whereas the phosphoric acid and poly(phosphoric acid) are represented with thick sticks. With a further temperature increase to 1400 K, a clustering or polymerization of phosphoric acid molecules is observed accompanying the generation of a large quantity of water, indicating drastic tribochemical reactions, as shown in Figure 2c. The molecular configurations of aforementioned major products after sliding are shown in Figure 3.

On the other hand, when considering the interaction between phosphoric acid/water and quartz, the dominating interactions are the hydrogen bonds between the phosphoric acid/water and surface hydroxyls. Figure 2d,e,f shows the partial enlarged detail views corresponding to Figure 2a,b,c, respectively, indicating different types and strengths of the interfacial interactions at different temperatures: (a) at

dx.doi.org/10.1021/jp406360u | J. Phys. Chem. C 2013, 117, 25604–25614

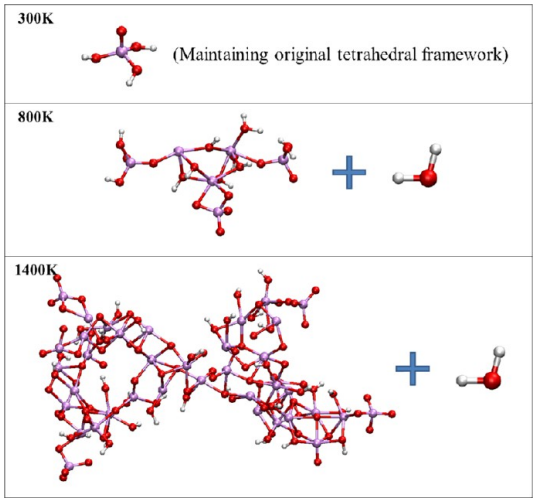

Figure 3. Major product after sliding: water; three transient molecular structures of the typical phosphoric/poly(phosphoric acid)s formed at 300, 800, and 1400 K. Several overcoordinated phosphorus and oxygen atoms correspond to intermediate or transition states during the dehydration or hydration process under high temperature/pressure conditions.

relatively lower temperatures, only phosphoric acid/surface hydrogen bonds exist; (b) with temperature rising, water molecules are produced and mainly accumulated near the surface with decreasing phosphoric acid/surface and emergence of water/surface hydrogen bonds; (c) at relatively higher temperatures, almost only water/surface hydrogen bonds exist but with much less quantity. Therefore, it can be envisioned that the tribochemical reaction may modify the type and strength of lubricant hydrogen bonding to surface, and the greater the degree of tribochemical reaction, the greater the number of water hydrogen bonding to surface. Based on such observations, it is tempting to speculate that the change in hydrogen bond interaction will lead a change in friction, which will be discussed later.

Figure 4a shows the time evolution of cumulative averaged friction coefficients at different temperatures. For each temperature, it takes about 100 ps for the friction coefficient to become stable. Therefore, in our study, the term "steady-state friction coefficient" refers to the average friction coefficient from 100 to 800 ps where the friction coefficient maintains stability. On the whole, the steady-state friction coefficients decrease rapidly from ~0.3 to ~0.02 as temperatures increase from 300 to 1400 K, although there exists some irregularity around 1000 K. Very low steady-state friction coefficient ($\mu \approx 0.02$) could be reached when the temperature goes up to 1400 K, close to the so-called superlubricity regime. The decrease of friction coefficient with increasing temperature could be explained by the enhanced translational and rotational

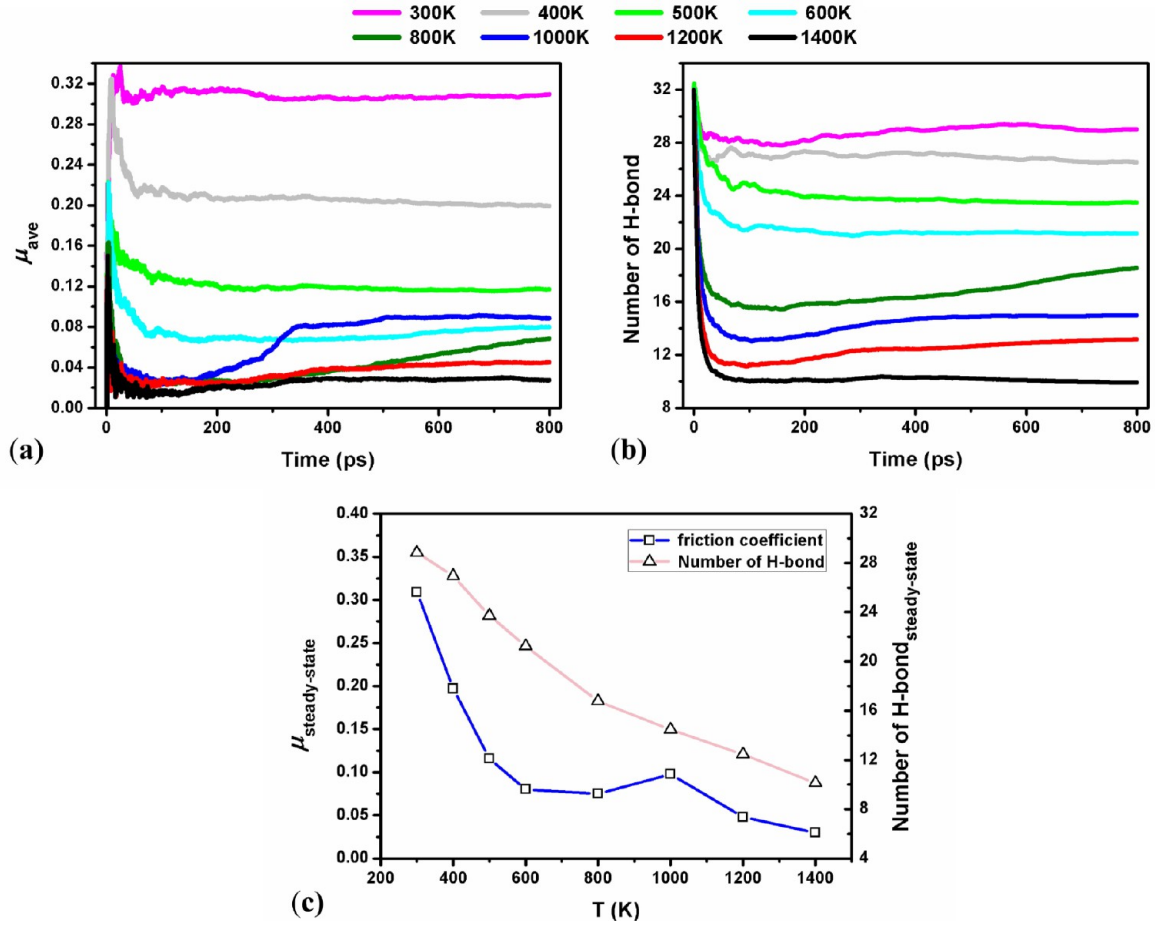

Figure 4. (a) Cumulative averaged friction coefficient. (b) Cumulative averaged number of hydrogen bonds between lubricant and substrate. (c) Friction coefficient and number of hydrogen bonds in steady state. The friction coefficient was calculated from the force acting on the fixed layer of lower substrate. The number of hydrogen bonds was calculated between lower substrate and lubricant atoms.

dx.doi.org/10.1021/jp406360u | J. Phys. Chem. C 2013, 117, 25604−25614

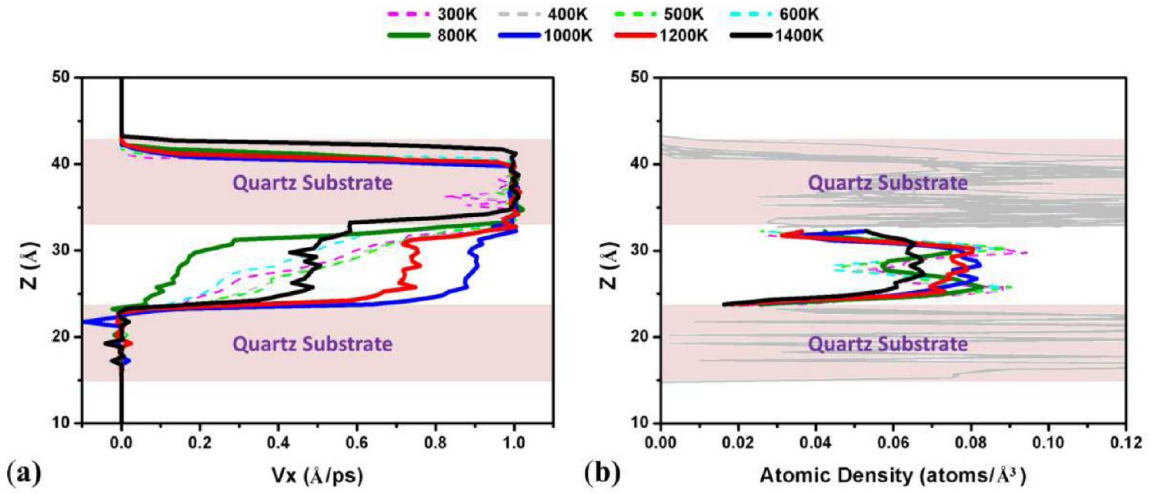

Figure 5. (a) Atom velocity profiles in the sliding direction (x direction) for different temperatures. (b) Atomic density profiles for different temperatures. These values were averaged over all atoms within 0.5 Å thick slabs across the z dimension in the steady-state friction period, where the z-axis corresponds to the quartz surface normal. The red shadows symbolize the quartz substrate region. For the sake of clarity, the atomic density in the substrate region is represented by a gray solid line.

motion of the phosphoric acid molecules and tribochemical reactions in low (300−600 K) and high (800−1400 K) temperature ranges, respectively, which will be further discussed in sections 3.2 and 3.3.

The interfacial friction is mainly governed by the atomic structures and interatomic interactions at the sliding interface. So before investigating the low friction mechanism, we first learn the relationship between the friction coefficient and the interfacial interactions quantitatively. The interaction between phosphoric acid molecules and quartz surfaces could be categorized into three types based on the bonding strength, namely van der Waals interactions, hydrogen bonds, and covalent bonds. A distance-dependent scheme is employed to classify these interactions, similar to that used in an atomistic system including phosphoric acid derivative and silica surface.[50] The results revealed that there are no covalent bonds at the relatively lower temperatures ($300 \leq T \leq 600$ K), while there are few instantaneous covalent bonds (≤ 2) at the relatively higher temperatures ($800 \leq T \leq 1400$ K). The hydrogen bonds are considered to have the largest contribution to friction between lubricant and quartz surface. As shown in Figure 1, the hydroxyl groups on quartz surface and in phosphoric acid molecules form a complicated interfacial hydrogen bond network. With the relative sliding, it is observed that the hydrogen bond network are destroyed and rebuilt dynamically. The correlativity between number of hydrogen bond and friction is investigated. The total number of hydrogen bonds between lubricant molecules and lower substrate is computed every step and then accumulated and averaged in the similar way as friction coefficient calculation. Figure 4b shows the evolution of the number of hydrogen bonds on interface between lubricant and substrate. The number of hydrogen bonds decreases as the system temperature increases from 300 to 1400 K, which is the same as the variation tendency of friction coefficient. The results reveal the strong positive correlativity between the friction coefficient and the number of interfacial hydrogen bonds.

Such a remarkable change in tribological performance also indicates qualitative changes in atomic configurations and velocity accommodation mode. So distributions of atom velocity and density at different temperatures are also examined, as shown in Figures 5a and 5b, respectively. The upper substrate moves with a velocity of 1.0 Å/ps in the sliding direction, while the lower substrate stays in the original position. When the temperature ranges from 300 to 600 K, the density profiles of the phosphoric acid present two well-defined peaks, and velocity shows a Newtonian fluid-like behavior. However, when the temperature ranges from 800 to 1400 K, the lubricant shows more and more homogeneous density profile and the lubricant atoms tend to move together with almost the same speed, while the abrupt change of velocity near the quartz surface suggests the emergence of a slip plane. The existence of slip plane with weak interfacial interaction is usually a prerequisite for achieving ultralow friction in solid lubrication cases.[34]

3.2. Dynamics of Phosphoric Acid Molecules. In nanotribology, the dynamics of molecule was considered one of the key factors for friction. In the literature, it is reported that the motion type, whether translational or rotational, will greatly influence the interaction between carbon nanotubes.[66] Moreover, high efficiency in lubricants consisting of small molecules is generally due to their excellent fluidity which depends crucially on their fast dynamics. Leng et al. have demonstrated that the origin of persistent fluidity of the confined water is closely associated with their rotational dynamics, accompanied by fast translational diffusion.[64] Similar to water, the dynamics of phosphoric acid molecules could also be dominated by their rotation and diffusion. As mentioned above, when $300 \leq T \leq 600$ K, there was no occurrence of tribochemical reactions, and the phosphoric acid molecules maintained their tetrahedral structure. Hence, in this temperature range, the origin of good lubrication performance of phosphoric acid can be probed by examining their rotational and translational dynamics. In this subsection, the rotation and diffusion calculations are performed in static state (no shearing). And the first 100 ps of simulation is discarded in these dynamics analysis to ensure equilibration.

We first study the reorientation rates which are derived from the relaxation time of the correlation functions. Figure 6 shows stretched exponential fits to the reorientational correlation

dx.doi.org/10.1021/jp406360u | J. Phys. Chem. C 2013, 117, 25604−25614

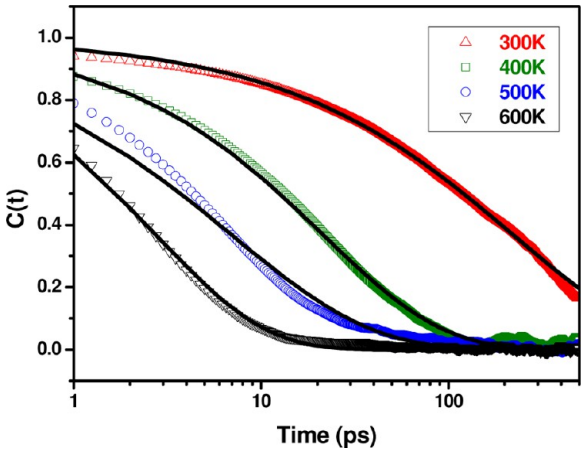

Figure 6. Stretched exponential fits to the reorientational correlation functions for PO groups in phosphoric acid. The black solid lines are the fitted KWW stretched exponential functions, and the scatter symbols are the calculated reorientational correlation functions from MD simulations.

functions for PO groups in phosphoric acid. The fitting parameters and correlation time for various temperatures are listed in Table 1. The result underlines that these reorientational correlation time are strongly temperature dependent; namely, with increasing system temperature they encounter a pronounced decay. The reorientation rate λ—the inverse of reorientational correlation time τ_μ—increases 100-fold from 0.003 to 0.304 ps^{-1}, corresponding to a strong acceleration of rotational motion.

Table 1. Reorientational Correlation Times and Diffusion Coefficients of PA at Different Temperatures

T (K)	τ (ps)	γ	τ_μ (ps)	λ (ps^{-1})	D ($Å^2$/ps)	$MSD_{350\ ps}$ ($Å^2$)
300	221.631	0.600	333.395	0.003	0.006	4.139
400	21.476	0.680	27.982	0.036	0.024	13.368
500	6.959	0.582	10.909	0.092	0.140	62.234
600	2.749	0.745	3.291	0.304	0.917	314.160

We also examined the translational dynamics of phosphoric acid molecules. Given the confined and inhomogeneous geometry of this fluid, we calculate the mean-square displacement (MSD) of phosphoric acid molecules and phosphorus atoms in the lateral $x-y$ direction.[64] To get better statistics, the ensemble average of MSD is calculated using multiple time origins as represented in the Methods and Models section, and only the first half of the mean-squared displacement (i.e., 0–350 ps) is considered when determining the diffusion coefficient. The corresponding diffusion coefficients D are listed in Table 1. It is shown that the diffusion coefficient of phosphoric acid increases sharply from 0.006 to 0.917 $Å^2$/ps when the system temperature rise from 300 to 600 K. In addition, diffusional behavior can be compared qualitatively by direct comparison of the magnitude of the MSDs at 350 ps: diffusion of phosphoric acid molecules is promoted roughly 80-fold (from 4.139 to 314.160 $Å^2$) when temperature increases from 300 to 600 K. This shows that temperature rising can strongly promote the translational motion of phosphoric acid even under the confinement.

Overall, the above findings provide a strong indication that the accelerated dynamics of phosphoric acid molecules is likely to be responsible for the corresponding friction reduction, when the system temperature increases from 300 to 600 K. It is generally accepted that the dynamics of molecules located in hydrogen bond network is related to hydrogen bond relaxation; namely, the fast molecule motion is corresponding to the short hydrogen bond lifetime, and vice versa.[67,68] Specifically, when molecules are bound to the surface via hydrogen bonds, their dynamics will be greatly hindered.[69,70] Therefore, we can deduce that the accelerated dynamics of phosphoric acid molecules under confinement with increasing interfacial temperature will lead to a weaker and less stable hydrogen bond network with shorter mean lifetime. In the case of our simulations, that leads to a reduction of the quantity of interfacial hydrogen bonds and friction.

3.3. Tribochemical Reactions. Based on the results presented above, it can be deduced that the appearance of slip plane, in conjunction with a complicated tribochemical process, may contribute to the friction reduction, when the system temperature rise from 800 to 1400 K. Here, we have given a detailed discussion on the corresponding tribochemical reaction mechanism. It is known that poly(phosphoric acid) can be obtained by condensation of several phosphoric acids by elimination of water, the chemical formula of which is

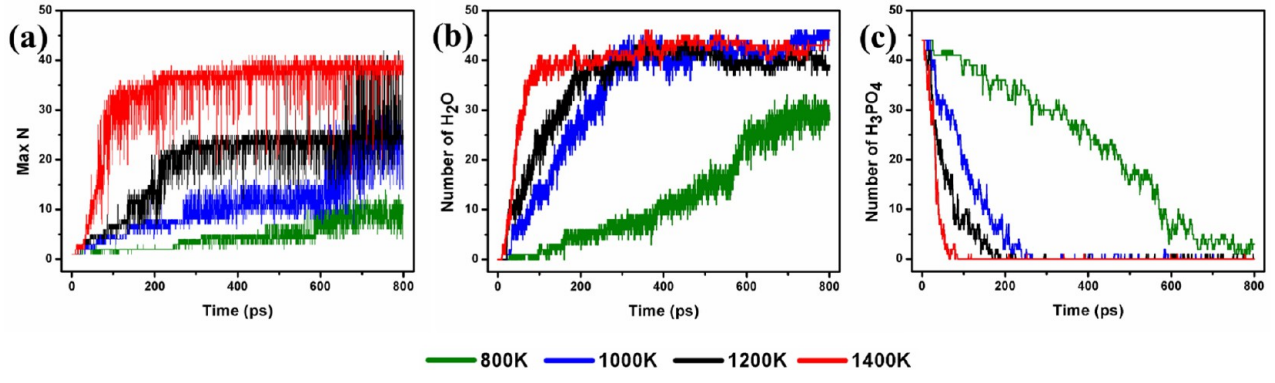

Figure 7. (a) Max N (number of phosphorus atoms in the largest poly(phosphoric acid) in the system) versus simulation time for various temperatures; the fluctuation indicates that the tribochemical reaction achieves dynamic equilibrium, especially for the 1400 K case where the break of a single macromolecule into two or more fragments or their recombination into one macromolecule could cause abrupt decrease/increase in max N. (b) Number of water molecules versus simulation time for various temperatures. (c) Phosphoric acid decay versus simulation time for various temperatures.

dx.doi.org/10.1021/jp406360u | J. Phys. Chem. C 2013, 117, 25604–25614

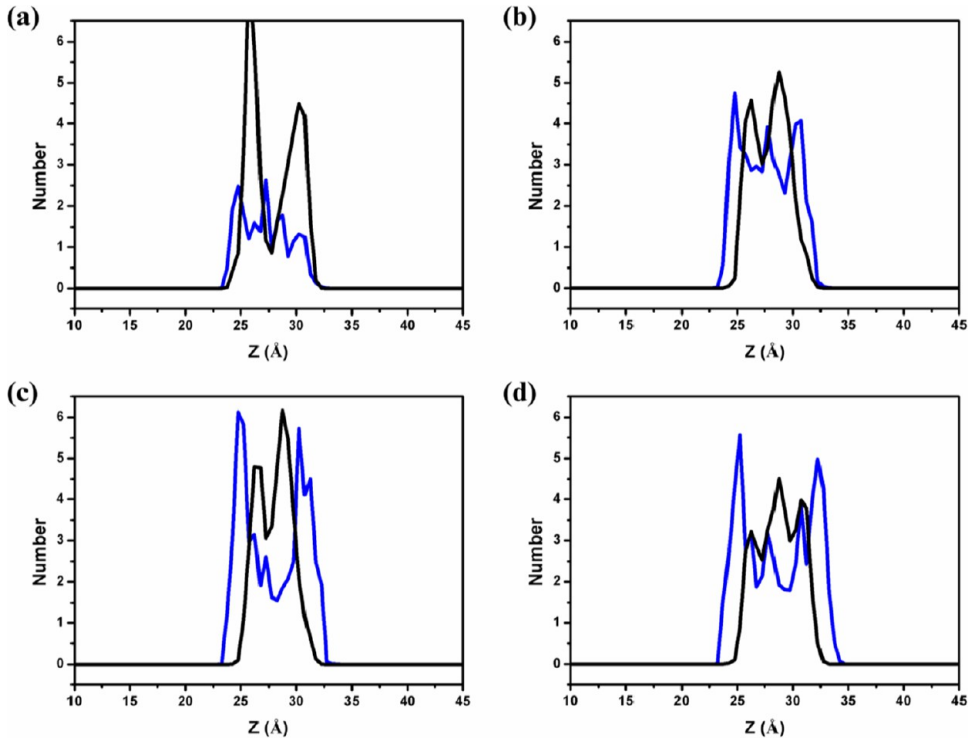

Figure 8. Number profiles of water oxygen atoms (blue) and phosphorus atoms (black) along the surface normal direction (Z). The number profiles are averaged during steady-state friction period. At temperatures (a) 800 K and (b) 1000 K, water distribution along the surface normal is relatively homogeneous. At temperatures (c) 1200 K and (d) 1400 K, water distribution exhibits two well-defined peaks between the phosphorus peak and the silica substrates, which indicates formation of lubricating water films between poly(phosphoric acid) layer and solid surface.

$H(HPO_3)_nOH$ ($n > 1$), so water should be present after the dehydration reaction.[71,72] For example, the dehydration process to obtain pyrophosphoric acid is as follows:

$$2H_3PO_4 \rightarrow H_4P_2O_7 + H_2O \quad (10)$$

From the snapshots shown in Figure 2, polymerization of adjacent phosphoric acid molecules and generation of poly(phosphoric acid)s are observed. Quantitative analysis on the tribochemical processes is further given in detail. Figure 7a shows the time evolution of the max N (number of phosphorus atoms in the largest polymer $H(HPO_3)_nOH$ in the system), which is a sign of the degree of polymerization in the current system. It is clear that during the shear process the size of the polymer generally increases with time with a certain fluctuations. It is assumed that this poly(phosphoric acid) is one of the main compositions of the gel-like film found experimentally in the sliding track by Li.[5] In addition to poly(phosphoric acid), the major species identified are water and phosphoric acid. Figure 7b,c shows time evolution of the total number of H_3PO_4 and H_2O, indicating a consumption of phosphoric acid molecules and a production of water molecules during the tribochemical process.

It is also important to note that temperature plays an important role in the tribochemical reactions. From Figure 7a, it is observed that after 800 ps the size of the largest polymer increases with temperature, indicating an enhanced polymerization with rising temperature, which could result in an even single macromolecule at 1400 K. The typical molecular network of poly(phosphoric acid)s formed at 800 and 1400 K is shown in Figure 3. And it is also clear from Figure 7a−c that the reaction rate increases with temperature with a faster consumption of reactant (phosphoric acids) and formation of product (poly(phosphoric acid)s and water). Once the reaction has equilibrated, totally 44 phosphoric acid molecules have consumed, while 42 ± 2 water molecules have formed. Therefore, the ratio of phosphoric acid consumed to water formed is approximately 1:1. Based on the above analysis, the tribochemical reactions can be roughly described as follows, where γ represents shear strain and ΔT represents temperature rise induced by friction:

$$nH_3PO_4 \xrightarrow{\gamma,\Delta T} (HPO_3)_n + nH_2O \quad (11)$$

It is tempting to speculate that it is this polymerization process increasing the degree of chemical connectivity that leads to the aforementioned change of velocity accommodation mode. More importantly, we note that the water distribution in the interface region is crucial for low friction. As shown in Figure 8, when temperature is 800 and 1000 K, not only is the quantity of water molecules smaller (for 800 K), but their distribution along the surface normal is relatively homogeneous. In these cases, the friction coefficient indeed exhibits an increasing tendency (Figure 4a). Interestingly, for 1200 and 1400 K, the distribution of water molecules exhibit two well-defined peaks between poly(phosphoric acid) layer and solid surface, while the friction coefficient keeps decreasing to 0.02, which indicates formation of lubricating water films. One important factor to result in the difference in the water distribution is the polymerization degree, which can be described by max N in Figure 7. With enhanced polymerization, the separation between poly(phosphoric acid) and water molecules becomes more obvious, until the complete segregation of the two phases and formation of one single polymer. During this process, the water molecules would no longer be constrained in between the polymer fragments by the

dx.doi.org/10.1021/jp406360u | J. Phys. Chem. C 2013, 117, 25604−25614

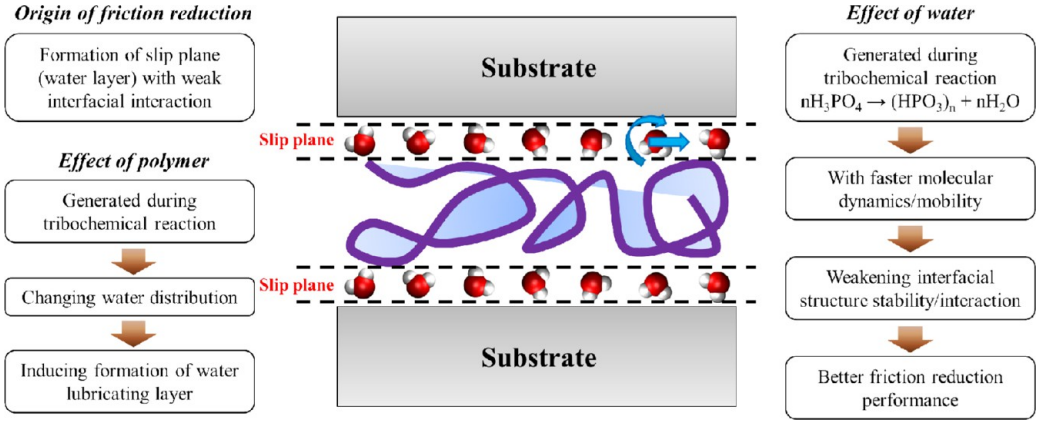

Figure 9. Schematic of tribochemical mechanism of friction reduction.

hydrogen bond network, but rather accumulate at the sliding interface and form a lubricating layer. Water molecules are much smaller than phosphoric acid molecules, so their dynamics will be faster. That will contribute to an even weaker and less stable interfacial hydrogen bond network as shown in Figure 4 and hence a lower friction. Similar behavior of water is also found in the amorphous carbon (a-C)/glycerol system,[41] so the friction reduction mechanism by production of water molecules reported here is general, not specifically for the silica/phosphoric acid system.

It should be mentioned that due to the time scale limitations of MD method, it is common to perform frictional sliding simulation with much higher velocities than experimental ones up to now, such as 100 m/s used in this study. In order to obtain a brief knowledge of the effect of high sliding velocity, we also test velocity of 10 m/s in a set of separated simulations at different temperatures. The qualitative findings about tribochemistry still hold, namely the existence of threshold for tribochemical reaction to take place and the correlation between friction, temperature, and hydrogen bond network remains unchanged. So the main conclusions drawn here are not limited to very high shear rate regime. Detailed behavior and mechanism of velocity dependence on friction and tribochemistry will be learned and presented in future studies.

3.4. Discussion of Mechanism of Friction Reduction. It is worth noting that underlying mechanisms of friction reduction both in the lower and higher temperature regimes are not isolated but unified, though with totally different interfacial structures and velocity accommodation modes. It is revealed that a weaker and less stable interfacial hydrogen bond interaction corresponding to a faster interfacial molecular mobility/dynamics will lead to a further decreasing friction.

There indeed are some previous works concerning the effects of hydrogen bond on friction. One of the remarkable works was done by Chen et al.;[73] their main finding is that friction decreases with velocity in systems that are capable of forming cross-linked networks of H-bonds at the interface with linkage energies that are easy to overcome at the applied loads. They explain the results with a model with the domains of glassy H-bond networks: At a certain critical value of the applied stress, the H-bonds break, causing a local "melting" of the network and slippage of the interface; At low velocity, after stress release by the slip event, domains of H-bond networks can re-form by nucleation and growth until they become large enough to arrest the motion. If the sliding velocity is too high, reorganization will not be complete, leading to a less stable interface structure and a smaller friction force. So their finding is consistent with ours to a large extent; namely, a less stable interface structure will lead to a smaller friction force.

Interestingly, H-bond breaking and re-formation have also been discussed in the context of protein unfolding, which determines the strength of the H-bonds network and the mechanical resistance.[74,75] In these works, by applying basic thermodynamics concepts from fracture mechanics to the protein unfolding problem and using large-scale full-atomistic MD simulation, authors provide a prediction and explanation for the intrinsic shear strength limit of protein, considering the interplay between entropic elasticity and the H-bond dissociation energy. In addition, Erbas et al. have found that friction between hydrogen-bonded matter obeys a simple law in which the friction force is proportional to the number of H-bonds.[76] In this context, the strong positive correlativity between friction and the number of interfacial hydrogen bonds, which is found in our study, is generally valid.

In our cases, there are H-bonds formed and disrupted dynamically between substrate surface and lubricant molecules (phosphoric acid at lower temperature and water at higher temperature) during sliding. From our simulation results, although phosphoric acid is not a good lubricant at 300 K, it does lubricate the system to a certain extent at 400−600 K as shown in Figure 4, where tribochemical reactions do not take place. Meanwhile, the mobility/dynamics of phosphoric acid increase obviously as shown in Table 1. These results in the lower temperature range show the significance of mobility/dynamics of the phosphoric acid molecules on the stability of hydrogen bond network and friction. Moreover, the production of water molecules during the tribochemical process in the higher temperature range will further decrease friction, as shown in Figure 9. We explain this phenomenon by the difference in mobility/dynamics of different molecules, since water has much faster rotational and translational motion with smaller molecular size than phosphoric acid. As the mobility/dynamics of these lubricant molecules becomes faster, the mean lifetime of the corresponding interfacial H-bonds becomes shorter, indicating a weaker interfacial H-bond structure and hence a lower friction.

4. CONCLUSIONS

Reactive molecular dynamics simulations are conducted to investigate the superlubricity mechanism induced by tribochemical reactions in the silica/phosphoric acid system. The sliding friction behaviors and tribochemistry of phosphoric acid

dx.doi.org/10.1021/jp406360u | J. Phys. Chem. C 2013, 117, 25604−25614

under solid confinement and shear have a strong temperature dependence in a wide temperature range. At relatively lower temperature range ($300 \leq T \leq 600$ K), the rotational dynamics and translational diffusion of phosphoric acid molecules are accelerated with increasing interfacial temperature. As a result, a weaker and less stable interfacial hydrogen bond network with shorter mean lifetime could lead to a reduction of the quantity of interfacial hydrogen bonds and friction. At relatively higher temperature range ($800 \leq T \leq 1400$ K), the tribochemical reactions which are characterized by polymerization of phosphoric acid molecules, generation of water molecules, and formation of slip planes are also enhanced by increasing temperature.

The variation of hydrogen bond interaction strength and change of velocity accommodation mode are found to have important relation with friction. The generation of water molecules and their accumulation at the sliding interface are observed, which could lead to an even weaker interfacial hydrogen bond interaction due to the much faster dynamics of water molecules and hence show good lubricating properties with a friction coefficient as low as 0.02. This study sheds light on a general understanding of the water-based superlubricity mechanism.

AUTHOR INFORMATION

Corresponding Author

*Phone +861062788310; e-mail mtb@mail.tsinghua.edu.cn.

Notes

The authors declare no competing financial interest.

ACKNOWLEDGMENTS

We thank Prof. Y. S. Leng of GWU and Dr. J. J. Li of SKLT for helpful suggestions and discussions. This work is financially supported by the National Natural Science Foundation of China (Grants 51005129, 51075226, and 51027007) and the Young Talents Program of China. A.C.T.v.D. and J.Y. acknowledge funding from the US National Science Foundation/SI2 Grant 1047857. Computations were carried out on the Tsinghua National Laboratory for Information Science and Technology.

REFERENCES

(1) Mosey, N. J.; Muser, M. H.; Woo, T. K. *Science* **2005**, *307*, 1612.
(2) Martin, J. M. *Tribol. Lett.* **1999**, *6*, 1.
(3) Spikes, H. *Tribol. Lett.* **2004**, *17*, 469.
(4) Nicholls, M. A.; Do, T.; Norton, P. R.; Kasrai, M.; Bancroft, G. M. *Tribol. Int.* **2005**, *38*, 15.
(5) Li, J.; Zhang, C.; Luo, J. *Langmuir* **2011**, *27*, 9413.
(6) Hirano, M.; Shinjo, K. *Phys. Rev. B* **1990**, *41*, 11837.
(7) Shinjo, K.; Hirano, M. *Surf. Sci.* **1993**, *283*, 473.
(8) Martin, J. M. Superlubricity of Molybdenum Disulfide. In *Superlubricity*; Erdemir, A., Martin, J. M., Eds.; Elsevier B.V.: Oxford, UK, 2005.
(9) Hsu, S. M. *Tribol. Int.* **2004**, *37*, 537.
(10) Hsu, S. M. *Tribol. Int.* **2004**, *37*, 553.
(11) Li, B.; Wang, X.; Liu, W.; Xue, Q. *Tribol. Lett.* **2006**, *22*, 79.
(12) Asay, D. B.; Dugger, M. T.; Ohlhausen, J. A.; Kim, S. H. *Langmuir* **2008**, *24*, 155.
(13) Barnette, A. L.; Asay, D. B.; Kim, D.; Guyer, B. D.; Lim, H.; Janik, M. J.; Kim, S. H. *Langmuir* **2009**, *25*, 13052.
(14) Morita, Y.; Onodera, T.; Suzuki, A.; Sahnoun, R.; Koyama, M.; Tsuboi, H.; Hatakeyama, N.; Endou, A.; Takaba, H.; Kubo, M.; Del Carpio, C. A.; Shin-yoshi, T.; Nishino, N.; Suzuki, A.; Miyamoto, A. *Appl. Surf. Sci.* **2008**, *254*, 7618.
(15) Li, K.; Amann, T.; Walter, M.; Moseler, M.; Kailer, A.; Ruhe, J. *Langmuir* **2013**, *29*, 5207.
(16) Li, J.; Liu, Y.; Luo, J.; Liu, P.; Zhang, C. *Langmuir* **2012**, *28*, 7797.
(17) Li, J.; Zhang, C.; Sun, L.; Lu, X.; Luo, J. *Langmuir* **2012**, *28*, 15816.
(18) Li, J.; Zhang, C.; Ma, L.; Liu, Y.; Luo, J. *Langmuir* **2013**, *29*, 271.
(19) Li, J.; Zhang, C.; Luo, J. *Langmuir* **2013**, *29*, 5239.
(20) Klein, J. *Friction* **2013**, *1*, 1.
(21) Onodera, T.; Morita, Y.; Suzuki, A.; Koyama, M.; Tsuboi, H.; Hatakeyama, N.; Endou, A.; Takaba, H.; Kubo, M.; Dassenoy, F.; Minfray, C.; Joly-Pottuz, L.; Martin, J.-M.; Miyamoto, A. *J. Phys. Chem. B* **2009**, *113*, 16526.
(22) Onodera, T.; Morita, Y.; Nagumo, R.; Miura, R.; Suzuki, A.; Tsuboi, H.; Hatakeyama, N.; Endou, A.; Takaba, H.; Dassenoy, F.; Minfray, C.; Joly-Pottuz, L.; Kubo, M.; Martin, J.-M.; Miyamoto, A. *J. Phys. Chem. B* **2010**, *114*, 15832.
(23) Mosey, N. J.; Woo, T. K.; Muser, M. H. *Phys. Rev. B* **2005**, *72*, 054124.
(24) Koyama, M.; Hayakawa, J.; Onodera, T.; Ito, K.; Tsuboi, H.; Endou, A.; Kubo, M.; Del Carpio, C. A.; Miyamoto, A. *J. Phys. Chem. B* **2006**, *110*, 17507.
(25) Haw, S. M.; Mosey, N. J. *J. Chem. Phys.* **2011**, *134*, 014702.
(26) Haw, S. M.; Mosey, N. J. *J. Phys. Chem. C* **2012**, *116*, 2132.
(27) Carkner, C. J.; Mosey, N. J. *J. Phys. Chem. C* **2010**, *114*, 17709.
(28) Stefanov, M.; Enyashin, A. N.; Heine, T.; Seifert, G. *J. Phys. Chem. C* **2008**, *112*, 17764.
(29) Harrison, J. A.; Brenner, D. W. *J. Am. Chem. Soc.* **1994**, *116*, 10399.
(30) Perry, M. D.; Harrison, J. A. *J. Phys. Chem.* **1995**, *99*, 9960.
(31) Harrison, J. A.; White, C. T.; Colton, R. J.; Brenner, D. W. *Thin Solid Films* **1995**, *260*, 205.
(32) Tutein, A. B.; Stuart, S. J.; Harrison, J. A. *Langmuir* **2000**, *16*, 291.
(33) Mikulski, P. T.; Harrison, J. A. *J. Am. Chem. Soc.* **2001**, *123*, 6873.
(34) Chateauneuf, G. M.; Mikulski, P. T.; Gao, G. T.; Harrison, J. A. *J. Phys. Chem. B* **2004**, *108*, 16626.
(35) Mo, Y.; Turner, K. T.; Szlufarska, I. *Nature* **2009**, *457*, 1116.
(36) Schall, J. D.; Gao, G.; Harrison, J. A. *J. Phys. Chem. C* **2010**, *114*, 5321.
(37) Ma, T. B.; Hu, Y. Z.; Wang, H. *Carbon* **2009**, *47*, 1953.
(38) Qi, Y.; Cheng, Y.; Cagin, T.; Goddard, W. A., III *Phys. Rev. B* **2002**, *66*, 085420.
(39) Zhang, Q.; Qi, Y.; Hector, L. G., Jr.; Cagin, T.; Goddard, W. A., III *Phys. Rev. B* **2005**, *72*, 045406.
(40) Matta, C.; Joly-Pottuz, L.; De Barros Bouchet, M. I.; Martin, J. M.; Kano, M.; Zhang, Q.; Goddard, W. A., III *Phys. Rev. B* **2008**, *78*, 085436.
(41) Martin, J. M.; De Barros Bouchet, M. I.; Matta, C.; Zhang, Q.; Goddard, W. A., III; Okuda, S.; Sagawa, T. *J. Phys. Chem. C* **2010**, *114*, 5003.
(42) van Duin, A. C. T.; Dasgupta, S.; Lorant, F.; Goddard, W. A., III *J. Phys. Chem. A* **2001**, *105*, 9396.
(43) van Duin, A. C. T.; Strachan, A.; Stewman, S.; Zhang, Q.; Xu, X.; Goddard, W. A., III *J. Phys. Chem. A* **2003**, *107*, 3803.
(44) Strachan, A.; van Duin, A. C. T.; Chakraborty, D.; Dasgupta, S.; Goddard, W. A., III *Phys. Rev. Lett.* **2003**, *91*, 098301.
(45) Chenoweth, K.; Cheung, S.; van Duin, A. C. T.; Goddard, W. A., III; Kober, E. M. *J. Am. Chem. Soc.* **2006**, *127*, 7192.
(46) Chenoweth, K.; van Duin, A. C. T.; Goddard, W. A., III *J. Phys. Chem. A* **2008**, *112*, 1040.
(47) Zhu, R.; Janetzko, F.; Zhang, Y.; van Duin, A. C. T.; Goddard, W. A., III; Salahub, D. R. *Theor. Chem. Acc.* **2008**, *120*, 479.
(48) Zhang, Q.; Cagin, T.; van Duin, A.; Goddard, W. A., III; Qi, Y.; Hector, L. G., Jr. *Phys. Rev. B* **2004**, *69*, 045423.
(49) Fogarty, J. C.; Aktulga, H. M.; Grama, A. Y.; van Duin, A. C. T.; Pandit, S. A. *J. Chem. Phys.* **2010**, *132*, 174704.

(50) Quenneville, J.; Taylor, R. S.; van Duin, A. C. T. *J. Phys. Chem. C* **2010**, *114*, 18894.
(51) Khalilov, U.; Neyts, E. C.; Pourtois, G.; van Duin, A. C. T. *J. Phys. Chem. C* **2011**, *115*, 24839.
(52) Manzano, H.; Moeini, S.; Marinelli, F.; van Duin, A. C. T.; Ulm, F.-J.; Pellenq, R. J.-M. *J. Am. Chem. Soc.* **2012**, *134*, 2208.
(53) Pitman, M. C.; van Duin, A. C. T. *J. Am. Chem. Soc.* **2012**, *134*, 3042.
(54) Hu, Y. Z.; Ma, T. B.; Wang, H. *Friction* **2013**, *1*, 24.
(55) Landman, U.; Luedtke, W. D.; Gao, J. *Langmuir* **1996**, *12*, 4514.
(56) Liu, Y.; Szlufarska, I. *Phys. Rev. Lett.* **2012**, *109*, 186102.
(57) Humphrey, W.; Dalke, A.; Schulten, K. *J. Mol. Graphics* **1996**, *14*, 33.
(58) Plimpton, S. *J. Comput. Phys.* **1995**, *117*, 1.
(59) Schneider; Stoll. *Phys. Rev. B* **1978**, *17*, 1302.
(60) Hayashi, K.; Tezuka, K.; Ozawa, N.; Shimazaki, T.; Adachi, K.; Kubo, M. *J. Phys. Chem. C* **2011**, *115*, 22981.
(61) Müller-Plathe, F. *J. Chem. Phys.* **1998**, *108*, 8252.
(62) Müller-Plathe, F. *Chem. Phys. Lett.* **1996**, *252*, 419.
(63) Wensink, E. J. W.; Hoffmann, A. C.; van Maaren, P. J.; van der Spoel, D. *J. Chem. Phys.* **2003**, *119*, 7308.
(64) Leng, Y. S.; Cummings, P. T. *Phys. Rev. Lett.* **2005**, *94*, 026101.
(65) Swenson, J.; Bergman, R.; Longeville, S. *J. Chem. Phys.* **2001**, *115*, 11299.
(66) Cook, E. H.; Buehler, M. J.; Spakovszky, Z. S. *J. Mech. Phys. Solids* **2013**, *61*, 652.
(67) Luzar, A.; Chandler, D. *J. Chem. Phys.* **1993**, *98*, 8160.
(68) Micali, N.; Trusso, S.; Vasi, C.; Blaudez, D.; Mallamace, F. *Phys. Rev. E* **1996**, *54*, 1720.
(69) Tamai, Y.; Tanaka, H.; Nakanishi, K. *Macromolecules* **1996**, *29*, 6761.
(70) Marchi, M.; Sterpone, F.; Ceccarelli, M. *J. Am. Chem. Soc.* **2002**, *124*, 6787.
(71) Tromp, R. H.; Spieser, S. H.; Neilson, G. W. *J. Chem. Phys.* **1999**, *110*, 2145.
(72) Spieser, S. A. H.; Leeflang, B. R.; Kroon-Batenburg, L. M. J.; Kroon, J. *J. Phys. Chem. A* **2000**, *104*, 7333.
(73) Chen, J.; Ratera, I.; Park, J. Y.; Salmeron, M. *Phys. Rev. Lett.* **2006**, *96*, 236102.
(74) Keten, S.; Buehler, M. J. *Phys. Rev. Lett.* **2008**, *100*, 198301.
(75) Keten, S.; Buehler, M. J. *Nano Lett.* **2008**, *8*, 743.
(76) Erbas, A.; Horinek, D.; Netz, R. R. *J. Am. Chem. Soc.* **2012**, *134*, 623.